White Rose Research Online

eprints@whiterose.ac.uk
https://eprints.whiterose.ac.uk
Universities of Leeds, Sheffield and York

Deposited via The University of York.

White Rose Research Online URL for this paper:
https://eprints.whiterose.ac.uk/id/eprint/220106/

Version: Published Version

Article:
Rahlff, Janina, Westmeijer, George, Weissenbach, Julia et al. (2024) Surface microlayer-mediated virome dissemination in the Central Arctic. Microbiome. 218. ISSN: 2049-2618

https://doi.org/10.1186/s40168-024-01902-0

Reuse
This article is distributed under the terms of the Creative Commons Attribution (CC BY) licence. This licence allows you to distribute, remix, tweak, and build upon the work, even commercially, as long as you credit the authors for the original work. More information and the full terms of the licence here: https://creativecommons.org/licenses/

Takedown
If you consider content in White Rose Research Online to be in breach of UK law, please notify us by emailing eprints@whiterose.ac.uk including the URL of the record and the reason for the withdrawal request.

UNIVERSITY OF LEEDS
University of Sheffield
UNIVERSITY of York

Microbiome

RESEARCH

Open Access

Surface microlayer-mediated virome dissemination in the Central Arctic

Janina Rahlff[1,2,3*], George Westmeijer[1], Julia Weissenbach[1], Alfred Antson[4] and Karin Holmfeldt[1]

Abstract

Background Aquatic viruses act as key players in shaping microbial communities. In polar environments, they face significant challenges such as limited host availability and harsh conditions. However, due to the restricted accessibility of these ecosystems, our understanding of viral diversity, abundance, adaptations, and host interactions remains limited.

Results To fill this knowledge gap, we studied viruses from atmosphere-close aquatic ecosystems in the Central Arctic and Northern Greenland. Aquatic samples for virus-host analysis were collected from ~60 cm depth and the submillimeter surface microlayer (SML) during the Synoptic Arctic Survey 2021 on icebreaker Oden in the Arctic summer. Water was sampled from a melt pond and open water before undergoing size-fractioned filtration, followed by genome-resolved metagenomic and cultivation investigations. The prokaryotic diversity in the melt pond was considerably lower compared to that of open water. The melt pond was dominated by a *Flavobacterium* sp. and *Aquiluna* sp., the latter having a relatively small genome size of 1.2 Mb and the metabolic potential to generate ATP using the phosphate acetyltransferase-acetate kinase pathway. Viral diversity on the host fraction (0.2–5 µm) of the melt pond was strikingly limited compared to that of open water. From the 1154 viral operational taxonomic units (vOTUs), of which two-thirds were predicted bacteriophages, 17.2% encoded for auxiliary metabolic genes (AMGs) with metabolic functions. Some AMGs like glycerol-3-phosphate cytidylyltransferase and ice-binding like proteins might serve to provide cryoprotection for the host. Prophages were often associated with SML genomes, and two active prophages of new viral genera from the Arctic SML strain *Leeuwenhoekiella aequorea* Arc30 were induced. We found evidence that vOTU abundance in the SML compared to that of ~60 cm depth was more positively correlated with the distribution of a vOTU across five different Arctic stations.

Conclusions The results indicate that viruses employ elaborate strategies to endure in extreme, host-limited environments. Moreover, our observations suggest that the immediate air-sea interface serves as a platform for viral distribution in the Central Arctic.

Keywords Surface microlayer, Polar, Phage, Lysogeny, Melt pond, Metagenomics, Bacteria, Viruses, Prophage induction, Auxiliary metabolic genes

*Correspondence:
Janina Rahlff
Janina.rahlff@uol.de
Full list of author information is available at the end of the article

© The Author(s) 2024. **Open Access** This article is licensed under a Creative Commons Attribution 4.0 International License, which permits use, sharing, adaptation, distribution and reproduction in any medium or format, as long as you give appropriate credit to the original author(s) and the source, provide a link to the Creative Commons licence, and indicate if changes were made. The images or other third party material in this article are included in the article's Creative Commons licence, unless indicated otherwise in a credit line to the material. If material is not included in the article's Creative Commons licence and your intended use is not permitted by statutory regulation or exceeds the permitted use, you will need to obtain permission directly from the copyright holder. To view a copy of this licence, visit http://creativecommons.org/licenses/by/4.0/. The Creative Commons Public Domain Dedication waiver (http://creativecommons.org/publicdomain/zero/1.0/) applies to the data made available in this article, unless otherwise stated in a credit line to the data.

Background

The Central Arctic Ocean is a remote and inhospitable region located in the Arctic Circle, encompassing the waters surrounding the North Pole. The region is characterized by harsh environmental conditions including cold temperatures, storms, ice and snow coverage, and extended periods of darkness (polar night) and light (midnight sun) in the Arctic winter and summer, respectively. Sea ice covers most of the area throughout the year posing significant challenges for scientific research and exploration. Sea ice coverage regulates the amount of sunlight reaching the surface of the ocean, consequently influencing primary productivity [1]. Since the Arctic region experiences rapid environmental changes due to climate change [2], understanding the Central Arctic and its ecosystems has become increasingly important. With forecasted globally rising temperatures, more sea ice will melt and net primary productivity will increase further [3, 4]. Viruses exert top-down control by infecting microorganisms and thus play a crucial role in aquatic ecosystems by influencing nutrient cycling and shaping microbial diversity [5, 6]. In general, viruses are understudied components of the Arctic Ocean and especially the Central Arctic Ocean (reviewed by [7]). This also applies to viruses in the upper 1 m of the ocean's surface including the < 1 mm surface microlayer (SML), where so-called neuston organisms reside [8, 9]. The lack of microbial and viral surveys from the immediate air-sea interface can be attributed to the fact that the typical CTD Niskin rosette water samplers cannot collect SML. However, the upper millimeters and meters of the Arctic Ocean are particularly affected by melting ice, which creates strong salinity gradients and introduces diverse sea-ice-associated biota into the oceanic water [10].

When sea ice melts, especially thin first-year ice, microbial biopolymers consisting of proteinaceous material can contribute to the formation of a gelatinous SML by accumulating at the air-sea boundary [11]. Polymeric gels at the air-water interface were previously detected in melt ponds [11], which are pools of melted water that form on the surface of sea ice, where they can make up approximately 50% of the surface area [12]. Viruses of bacteria (bacteriophages) have previously been isolated from Arctic sea ice [13, 14], but the fate of viruses in melt ponds remains unknown [10]. However, by accumulating in the skin layer between the ocean and atmosphere, the polymeric compounds and viruses can more easily end up in aerosols [15, 16] with the potential of nucleating ice and influencing cloud formation [17–19].

The Tara Oceans Global Circle expedition has increased our knowledge of viral populations around the Arctic Ocean [20]; however, investigations on viruses from the Central Arctic Ocean are missing. This especially includes omics-based investigations of the virioneuston (reviewed by [21]), which are lacking for the entire polar regions. Activity and abundance of virioneuston, compared to virioplankton, were found to be enhanced in the Arctic (Norwegian Sea and North of Svalbard) [22]. This suggests that viral lysis in the Arctic surface microlayer (SML), as opposed to other ecosystems like sea ice [23], can significantly contribute to the release of dissolved organic carbon, thereby promoting the growth of heterotrophic microbes. Consequently, bacterioneuston numbers were also higher in the Arctic Ocean SML compared to the underlying surface water (ULW) [24], and the SML of open water contained more bacteria than the SML of melt ponds [11]. With the increasing warming of the surface ocean due to ongoing climate change, bacterial production is enhanced, which in turn stimulates viral activity [25]. This is due to the tight coupling of viral and bacterial variations in the Nordic Seas, influenced by various abiotic factors such as water masses, latitude, and water pH [26]. During the Synoptic Arctic Survey 2021 expedition, we aimed to fill major knowledge gaps regarding diversity, replication cycle prevalence, host interactions, and dispersal patterns of DNA viruses by conducting samplings of the SML during our journey through the Central Arctic. We used metagenomics, cultivation, and prophage induction assays to gain insights into how Arctic viruses adapt to hosts in the boundary layer ecosystem influenced by melting ice and freeze-thaw cycles.

Methods

Sampling and water filtration

Samples were collected during the Synoptic Arctic Survey 2021 [27] exploring the Central Arctic Ocean, the North Pole, and Northern Greenland between July and September 2021 (see Table S1). Wind speed was measured at the sampling site using a handheld anemometer model MS6252A (Mastech Group, Brea, CA, USA). Water temperature and salinity were measured using a thermosalinometer, model Professional Plus, YSI (Xylem, Washington, D.C., USA). Sampling of the SML was conducted with a glass plate sampler [28] either from (a) a melt pond, (b) seawater sampled from the ice edge of a lead (Fig. 1b), and (c) from seawater reached from the lowered gangway of the icebreaker Oden. The glass plate was submerged perpendicularly to the water surface into the water and slowly withdrawn. The SML adheres to the glass and is collected from it by wiping off both sides of the plate with a squeegee blade into a collection bottle. The glass plate and bottle were cleaned with ethanol and pre-rinsed with sample water. This method is state-of-the-art for virioneuston sampling [29, 30].

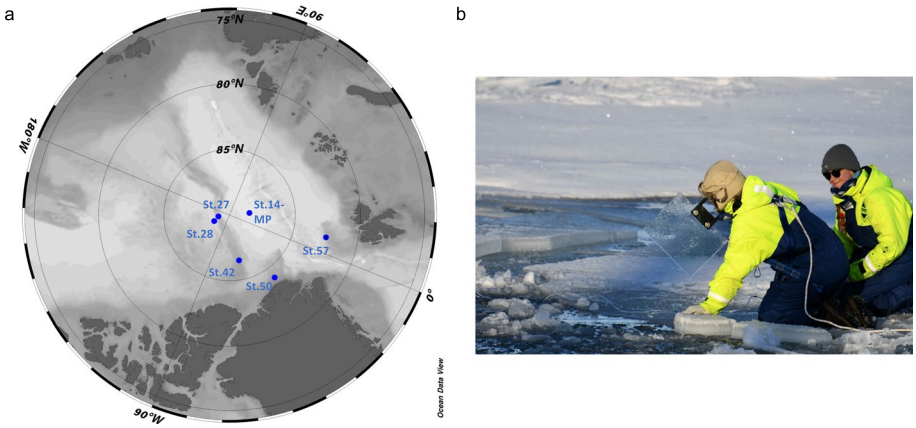

Fig. 1 Sampling the surface microlayer in the Central Arctic. Map showing stations of surface microlayer and underlying water sampling. There were five stations for oceanic sampling and one station labeled with "-MP" for a single melt pond station. Map was created with Ocean Data View [31] (**a**). Representative picture for sampling surface microlayer with the glass plate sampler from the ice edge (photo: Hans-Jørgen Hansen, MacArtney Underwater Technology) (**b**)

Sampling locations for the sporadic microlayer samplings are depicted in Fig. 1a. As a reference sample, ULW from ~60 cm depth was sampled using a 100 mL syringe connected to a hose. The syringe and the hose were rinsed with sample water and sterilized with 70% ethanol and Milli-Q water after use. Sample water was sequentially vacuum-filtered over a series of membranes featuring pore sizes of 5 µm and 0.2 µm (47 mm diameter, both Nuclepore™ track-etched polycarbonate membrane, Whatman, Maidstone, UK), and the flow-through was flocculated using iron (III) chloride ($FeCl_3$) solution [32]. A 10× higher concentration than in the original protocol of 10 mg $FeCl_3$ L^{-1} was chosen to recover more viruses as this concentration was recently recommended for freshwater [33], and SML samples were partly derived from freshwater (a melt pond) or affected by freshwater melting ice at the air-water boundary. The iron flocculates were filtered with a peristaltic pump onto 142 mm diameter, 1 µm pore-sized polycarbonate filters (Whatman). From Station 42 onwards, we had to switch to a 1 µm PTFE membrane (Omnipore, Merck Millipore, Darmstadt, Germany). Filters were stored on dry ice or at −80 °C until DNA extraction.

DNA extraction and metagenomic analysis of MAGs

DNA was extracted using the DNAeasy Power Soil Pro kit or the DNAeasy PowerMax Soil kit (Qiagen, Kista, Sweden) for 47 mm and 142 mm filters, respectively. When applying the PowerMax Soil kit, a subsequent ethanol precipitation step with glycogen from mussels (Roche Diagnostics, Basel, Switzerland) as the carrier molecule was performed. DNA concentration was measured on a Qubit® 2.0 Fluorometer (Invitrogen/ Life Technologies Corporation, Carlsbad, CA, USA). Short-read sequencing was performed by SciLifeLab (Solna, Sweden) using Illumina DNA PCR-free library preparation. Samples were sequenced on the NovaSeq6000 (NovaSeq Control Software 1.7.5/RTA v3.4.4) with a 151nt (Read1)-19nt (Index1)-10nt (Index2)-151nt (Read2) setup using "NovaSeqXp" workflow in "S4" mode on the flowcell. The Bcl to FastQ conversion was performed using bcl2fastq_v2.20.0.422 from the CASAVA software suite. The quality scale used is Sanger/phred33/Illumina 1.8+. Adapter trimming and quality control were conducted using bbduk as part of BBTools [34] under the application of contaminant filtering using the Illumina PhiX spike-in reference genome (phix174_ill.ref.fa) and the artificial contaminants file (sequencing_artifacts.fa). Sickle v.1.33 [35] was subsequently run in pe mode and -t sanger setting. mOTUs v.3.0.2 [36, 37] was used on trimmed reads with options -A (reports full taxonomy) -c (reports counts) -M (to save intermediate marker gene cluster count) for the taxonomic profiling of bacteria and archaea based on single-copy phylogenetic marker genes. Data were read sum normalized and analyzed in R v.4.0.3 [38] within R Studio using the packages phyloseq v.1.34.0 [39] and ggplot2 v.3.4.2 [40].

Binning of prokaryotic metagenome-assembled genomes (MAGs) from > 5 µm to 0.2–5 µm samples was conducted using CONCOCT v.1.1.0 [41] and MetaBAT v.2.12.1 [42] on MetaSPAdes v.3.15.3 [43] -derived scaffolds with a minimum length of 1000 bp. DAS_Tool v.1.1.3 [44] with the default threshold was used to obtain a dereplicated set of MAGs, and uBin v.0.9.14 [45] was used for subsequent manual refinement. MAGs underwent quality checks in CheckM2 v.0.1.3 [46], and their GC content, coding density, and genome size were obtained from CheckM v.1.1.3 [47]. Taxonomic assignment was performed by the classify_wf

in GTDB-Tk v.2.1.0 [48] with the database R207_v2. MAGs with estimated completeness and contamination scores of ≥ 70% and ≤ 10%, respectively, in either uBin or CheckM2 were considered for further analysis and dereplicated together with the isolate genomes (see below) in dRep v.3.4.0 [49] using default settings. Reads were mapped back to dereplicated MAGs and isolate genomes by using the --reorder flag in Bowtie v.2.4.5 to subsequently predict in situ replication rates at default thresholds in iRep v.1.1.7 [50] including a mismatch filtering step with a 2% error rate (-mm 3). To assess encoded metabolic potential of MAGs, eggNOG-mapper v.2.1.9 [51] with options --itype genome -m diamond --genepred prodigal was run on MAGs and bacterial isolate genomes (see below). To determine pathway completeness, the obtained functional annotation from the eggnog-mapper was used as input for the reconstruct tool as part of the Kyoto Encyclopedia of Genes and Genomes (KEGG) mapper. Read breadth on MAGs was used to decide if a MAG is present in the melt pond or open water station, namely if 90% of the genome had a coverage of at least 1 in at least one of the melt pond or open water stations. This was done after mapping with Bowtie 2 and mismatch (-m 3) filtration using mapped.py (https://github.com/christophertbrown/bioscripts/blob/master/ctbBio/mapped.py). We excluded potential contaminant bacteria from MAGs and isolates (see discussion in the supplement) from this analysis (labeled with a "C" in Table S2).

Mining of vOTUs from metagenomes

All samples were assembled using both MetaSPAdes v.3.15.3 and the Metaviral SPAdes option therein [43, 52]. Viruses were identified using VIBRANT v.1.2.1 [53] with the -virome option for the < 0.2 µm fraction, and VirSorter 2 [54] using -include-groups "dsDNAphage,ssDNA." Outputs or viral scaffolds were combined and filtered to a length of > 10 kb, mostly representing dsDNA viruses, and CheckV v.1.0.1 [55] was run for quality checks. The viral scaffolds with attributes "medium-quality," "high-quality," and "complete" were kept for further analysis. Thereafter, viral scaffolds underwent dereplication at the species level in VIRIDIC v.1.0 r3.6 [56], and only one representative per species cluster was kept (preferentially a circular scaffold; otherwise, the longest scaffold of a cluster). Some viral scaffolds were excluded as explained in the Supplement. The mean depth and breadth of the resulting viral operational taxonomic units (vOTUs) coverage were calculated after mapping reads to vOTUs using Bowtie2 v.2.4.5 with settings --mp 1,1 --np 1 --rdg 0,1 --rfg 0,1 --score-min L,0,-0.1 [57] for mapping of ≥ 90% identical reads and following conventions of [58]. A coverage of ≥ 75% (read breadth) of the viral genome was achieved by running the calcopo.rb script [59]. Coverages were analyzed using the 04_01calc_coverage_v3.rb script [45] and subsequently normalized to read depths. Moreover, vOTUs were analyzed using PhaBOX [60] to detect the proportion of phages and their replication style using PhaMer [61] and PhaTYP [62], respectively. All vOTUs were clustered to viral clusters (VC) at the genus level using vConTACT2 v.0.9.19 [63] together with a recent viral reference database (2 July 2022: https://github.com/RyanCook94/inphared/tree/b614bb92f31d55bfb0ab6180604e59838e492875) from INPHARED [64], and results were compiled using graphanalyzer v.1.5.1 [65]. PhaGCN v.2.0 was used to assign viral families to vOTUs [66, 67].

Auxiliary metabolic genes, host prediction, and correlations for dispersal

Auxiliary metabolic genes (AMGs) that correspond to Class I AMGs, as defined by [68], were identified using AnnoVIBRANT (https://github.com/AnantharamanLab/annoVIBRANT). After gene calling with Prodigal [69], the vOTUs were further annotated using DRAM-v v.1.4.6 [70] to find AMGs related to cryosurvival. Two of these AMGs, namely ice-binding-like [Pfam/InterPro database, PF11999.11] and glycerol-3-phosphate cytidylyltransferase *(tagD)* [Enzyme Commission number, EC:2.7.7.39] were subjected to a BLASTp analysis with a threshold of 1e-10 against the Ocean Gene Atlas [71, 72]. This analysis investigated the biogeography of protein homologs in surface water of the Tara Oceans Microbiome Reference Gene Catalog 2 + metaG Arctic Inside (OM-RGC_v2_metaG), and the corresponding transcriptomic dataset (OM-RGC_v2_metaT) , as well as the relationship between distribution and temperature. To explore virus-host interactions, vOTUs were matched to genomes from the "Sept_21_pub" database of the Integrated Phage Host Prediction (iPHoP) tool v.1.2.0 [73]. The database was supplemented with dereplicated MAGs and genomes of isolated strains (see below) from this study. For the iPHoP predictions, a confidence score cutoff of 90 was applied, and the host genus with the highest confidence score was selected for visualization within Cytoscape v.3.9.0 [74]. The presence of vOTUs at five different stations (including the melt pond) was assessed based on read breadth, which was correlated with the average coverage of the vOTU for all SML and ULW samples, respectively. The underlying assumption was that the higher the coverage of vOTUs at the air-sea interface, i.e., the more abundant they are in the SML, the more they are to be spread across the Arctic and detected at multiple stations, as they are likely aerosolized more easily from the SML.

Bacterial isolation and genome analysis

For bacterial isolation, 900 µL of seawater was added to 600 µL of 50% glycerol, inverted for mixing, and stored at −80 °C. In the home laboratory, the sample water-glycerol mix was spread onto Zobell agar plates (1 g yeast extract (BD), 5 g bacto-peptone (BD), 15 g bacto agar (BD), 800 mL specific water -see below-, 200 mL Milli-Q water). To account for the fact that bacteria came from different aquatic sources or are potentially adapted to strong salinity gradients in the SML due to melting sea ice, agar plates with different water sources of different salinities were used. This was achieved by either adding Milli-Q (MQ) water, Baltic Sea (Bal) water collected from the Linnaeus Microbial Observatory [75] or Arctic Ocean (Arc) water to the Zobell plates. Incubations were performed at room temperature and 4 °C. Colonies of different morphologies were picked and cleanly streaked thrice. Finally, all isolated bacteria were grown at room temperature in liquid Zobell prepared with either Arc or Bal or MQ water. Stocks from all bacterial strains were prepared with 600 µL of 50% glycerol (Sigma) and 900 µL of liquid overnight grown culture, and stored at −80 °C. DNA from overnight cultures of bacterial isolates was extracted using the E.Z.N.A Tissue DNA Kit (Omega Bio-tek, Norcross, GA, USA), eluted in 50 µL, quantified on the Qubit® 2.0 Fluorometer, and stored at −80 °C. In total, 13 bacterial isolates (Table S3) were sent for whole-genome Illumina sequencing to SciLifeLab (Solna, Sweden) using the same platform and flowcell as mentioned above. Reads were processed as mentioned above and assembled using SPAdes v.3.15.3 with option --isolate. Prophages in MAGs and isolate genomes were searched using VIBRANT v.1.2.1. CRISPR spacers in isolate genomes were searched for and extracted with the CRISPRcasFinder online tool [76] and matched to vOTUs from the metagenomes and viromes using a BLASTn-short algorithm with an 80% similarity threshold.

Prophage induction experiments

A prophage induction assay was performed for the bacterial strains *Psychrobacter* sp. Arc29, *Leeuwenhoekiella aequorea* Arc30, *Pseudoalteromonas distincta* Arc38, and *Flavobacterium frigidarium* Arc14 (the latter as control for a strain lacking prophages, Table S4). Due to the contamination issue when sampling SML and ULW from the gangway (see Supplement), we chose only these bacteria since they are known from the literature to be psychrophilic and/or marine bacteria. In a 48-well plate, mitomycin C (Roche Diagnostics) was added as prophage-inducing reagent [77] in triplicates in different final concentrations: 1 µg mL^{-1}, 0.5 µg mL^{-1}, 0.1 µg mL^{-1}, and no mitomycin C added to 500 µL of overnight grown bacterial culture. To monitor bacterial growth, the optical density at a wavelength of 600 nm (OD_{600}) on a FLUOstar® Omega Microplate Reader (BMG Labtech, Ortenberg, Germany) was measured once per hour. A significant OD drop under mitomycin C treatment compared to the negative control indicated prophage induction. At the end of the experiment, the culture liquid from the wells of induced prophage was collected, pooled, and subsequently filtered through a 0.2-µm syringe filter. The flow-through was further concentrated from 10 mL volume in an Amicon® Ultra-4 Centrifugal Filter 50 kDa unit (Merck Millipore) and stored at 4 °C. DNA was isolated from 1 mL of the concentrated supernatant using Wizard PCR DNA Purification Resin and Minicolumns (both Promega, Madison, WI, USA) as previously described [78]. A successful cross-pole infection of Arctic *Pseudomonas* sp. G11 with lysogenic *Pseudomonas* phage vB_PaeM-G11 isolated from an Antarctic strain was recently shown [79] and inspired us for a similar cross-infection experiment. The induced Arctic phages were tested on an *L. aequorea* strain CCUG 50091T [80] isolated from Antarctic seawater and ordered from the Culture Collection of the University of Gothenburg, Sweden.

Genomic analysis of the induced phage's genomes

Since VIBRANT found two prophages in the genome of *L. aequorea* Arc30, whole-genome sequencing of the DNA from independent prophage induction experiments was performed to determine the prophage identity in the supernatant after filtration on 0.2 µm pore-size syringe filter. From one of these experiments, half of the virus supernatant after the concentration step was digested with amplification-grade DNAse I (Invitrogen/Thermo Fisher Scientific, Waltham, MA, USA) for 10 min at 37 °C before DNA extraction to reduce host DNA contamination. Sequencing was done on a NOVASeq6000 platform by using the INVIEW Resequencing service of Eurofins Genomics (Ebersberg, Germany). After read trimming and QC as mentioned above, the phage genomes were assembled using MEGAHIT v.1.2.9 [81], and scaffolds with viral genes were identified using CheckV. To be able to assemble one of the induced phages' genomes, the trimmed reads had to be randomly reduced to 1% using seqtk v.1.4 (https://github.com/lh3/seqtk). A circular proteomic tree was built for the induced phages using ViPTree v.4.0 [82] including genomes of related phages suggested by the tool. Intergenomic similarities with related phages were further explored in VIRIDIC [56] and protein clustering in the VirClust web tool [83]. Gene prediction and annotations were performed as explained above for vOTUs. The genome of the phage Arctus_1 was circularized in Artemis v.18.1.0 [84] and visualized using Proksee [85]. The sliding window application (window

size 10,000, step size 100) within Proksee was used to investigate the GC content distribution of the genome. To check for the biogeography of the induced prophages, their genomes were BLASTed against the IMG/VR viral nucleotide database v.4 [86] with an e-value of 1e-5.

Transmission electron microscopy

Phage supernatants resulting from the prophage induction experiment were examined by transmission electron microscopy (TEM) using negative staining as in [57]. Phages were loaded on pre-discharged 200-mesh copper grids covered with carbon film (Agar Scientific Ltd., Stansted, UK) and stained with 2% (w/v) uranyl acetate. Images were taken with the FEI Tecnai 12 G2 BioTWIN microscope. Capsid diameter and tail length were measured from TEM images using ImageJ v.1.53t according to a previously published protocol [87].

Statistics

Unpaired, non-parametric Mann-Whitney *U*-test for comparing means of the Shannon-Wiener index was carried out in GraphPad Prism v.10. Before the correlation analysis of vOTU coverage with distribution at stations, outliers were removed using the Robust Regression and Outlier Removal (ROUT) method with $Q=1$, as recommended in [88] and implemented in GraphPad Prism v.10, where also linear regressions were drawn. Spearman *r* correlation coefficient was applied, and groups for the different stations were compared using the Kruskal-Wallis test with Dunn's multiple comparison test.

Results

Taxonomic profiling of prokaryotes

According to the taxonomic profiling, the melt pond was dominated by *Bacteroidota* and particularly by a *Flavobacterium* sp. [genome reference from mOTUs is ext_mOTU_v3_22321], which was phylogenetically related to the melt pond-derived *Nonlabens* sp. (MAG_04 from our study) (Fig. 2a, Fig. S1) and had a relative abundance of 60.1% and 35.1% in the 0.2–5 µm fraction of the SML and ULW, respectively. A relative abundance of 21.6% and 32.9% from SML and ULW of the same size fraction remained unassigned. Other OTUs with > 1% relative abundances in the melt pond SML and ULW samples from the 0.2–5 to > 5 µm fraction were *Oceanospirillaceae* species, *Cellvibrionales* species, *Betaproteobacteria* bacterium MOLA814, *Rickettsia* sp., *Octadecabacter arcticus*, *Pelagibacteraceae* species, and *Polaribacter* sp. (Table S5). Open water samples were overall more diverse, as the Shannon-Wiener index indicated, with a range of 1.1–2.3 ($n=4$) for the melt pond and a range for open water samples of 2.4–3.7 ($n=8$). The difference between the two means was significant (two-tailed Mann-Whitney *U*-test, *U* value = 0, $p=0.0040$, Fig. 2c). However, a clear limitation is that the four melt pond samples were just different filtered fractions from the same melt pond, thus only providing a first glance at the low diversity of bacteria in melt ponds. Arctic open water samples contained less *Bacteroidota* (max.= 16%) and more *Pseudomonadota* (max.= 37.1%) compared to the melt pond (*Bacteroidota* max.= 60.1%; *Pseudomonadota* max.=7.9%), but a similar number of unassigned taxa. While the melt pond was mainly dominated by a single *Flavobacterium* sp. up to 60.1%, open water samples contained up to 19.6% relative abundance of up to 45 different species of *Flavobacteriaceae*.

Metabolic insights and predicted replication rates from Arctic MAGs

A total of 182 metagenome-assembled genomes (MAGs) were binned and dereplicated to 68 MAGs (Table S6). After further exclusion of likely contaminants, this resulted in in 50 MAGs, of which three MAGs were assigned to archaea (phyla *Thermoproteota* and *Thermoplasmatota*). Others were assigned to the bacterial phyla *Actinomycetota* (5), *Bacteroidota* (19), *Proteobacteria* (18), SAR324 (2), and *Verrucomicrobiota* (3). From 13 bacterial isolates, 8 dereplicated genomes were assigned to *Bacteroidota* (3), *Pseudomonadota* (4), and *Bacillota* (1). The average estimated completeness of these genomes was 91 ± 8% (mean ± STD, $n=58$, Fig. S2a), and based on the metabolic potential, the archaeal MAGs clearly diverged from the bacterial MAGs (Fig. S2c). The estimated genome size was similar for both the MAGs in the melt pond and open water and was 2 Mbp on average (SD = 0.51, $n=58$, Fig. S2b). Predictions on the index of replication (iRep) indicated that none of the bacterial isolates and only five MAGs, i.e., *Nonlabens* sp. (MAG_04), *Polaromonas* sp. (MAG_07), a *Spirosomaceae* bacterium (MAG_08), *Aquiluna* sp. (MAG_09), and *Burkholderiaceae* bacterium (MAG_34), were actively replicating in the melt pond sampled at Station 14 (iRep range 1.4–2.2, Table S7). Of these, *Aquiluna* sp. had the highest coverage of reads (up to 123×) indicative of the genome's abundance. In open water samples, iRep values indicated replication indices for 46 MAGs. The highest values were found for *Polaribacter* sp. (MAG_101, iRep = 5.9 and 3.4 at Station 28 and 42), *Patiriisocius* sp. (MAG_75, iRep = 5.1–6.0 at Station 57), and a *Flavobacteriaceae* bacterium (MAG_123, iRep = 4.0–4.9 at Station 57). *Candidatus* Pelagibacter (MAG_10), a Gammaproteobacteria bacterium (MAG_161), and a *Porticoccaceae* bacterium (MAG_168) were abundant on various stations but not among the most active bacteria based on iRep predictions. The bacterial strain *L. aequorea* Arc30, isolated

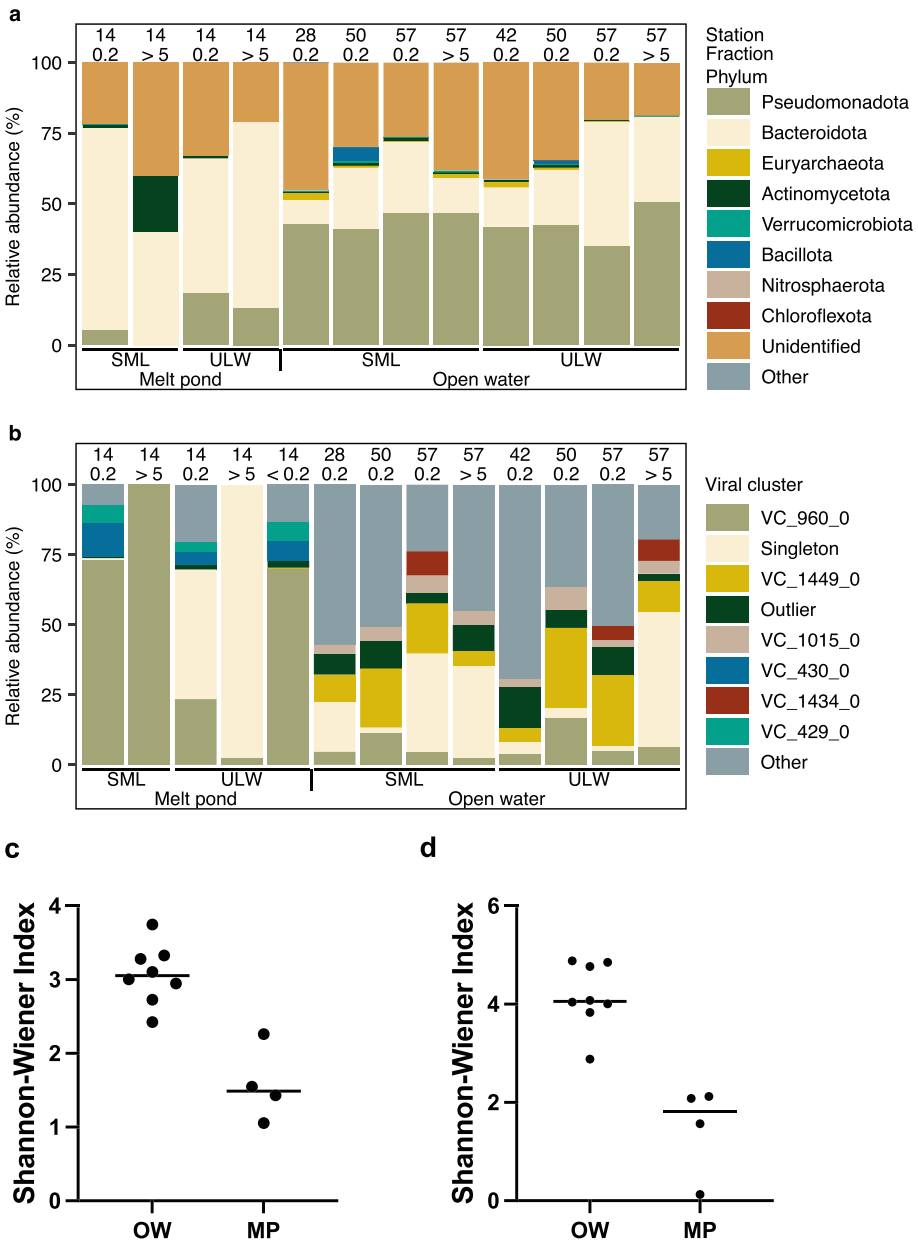

Fig. 2 Relative abundances of prokaryotes and viral clusters (VCs) in surface microlayer (SML) and underlying surface water (ULW) stations sampled across the Central Arctic. Community structure based on mOTUs depicting the eight most abundant prokaryotic phyla and unidentified ones while grouping the remaining phyla as "other" (**a**). Community structure of viruses based on VCs depicting the six most abundant VCs, singletons, and outliers while grouping the remaining VCs as "other". In vConTACT2, singletons and outliers are unclustered vOTUs and may present novel viruses (**b**). Fraction 0.2 refers to the filtered fraction between 0.2 and 5 µm pores-sized filter membranes, whereas fraction > 5 is the ≥ 5 µm pore size filtered sample. Fraction < 0.2 refers to the viral fraction. Alpha diversity of the mOTUs for melt pond (MP) and open water (OW) samples was estimated according to the Shannon-Wiener index for mOTUs (**c**) and vOTU communities (**d**). The line in the plot indicates the median

from the SML of Station 42, had a maximum coverage of 0.2×, indicating it was below the detection limit in the metagenomes and very low in abundance. Despite this, two prophages could be successfully induced from the isolate of this strain (see below). This low coverage also means that no predicted iRep value could be determined. Metabolic potential was analyzed for 29 MAGs, showing that in both the melt pond and open water heterotrophy prevailed due to the absence of the major carbon fixation pathways, and prokaryotes obtained their energy from the oxidation of organic compounds (Fig. 3). Taxonomic profiling of the

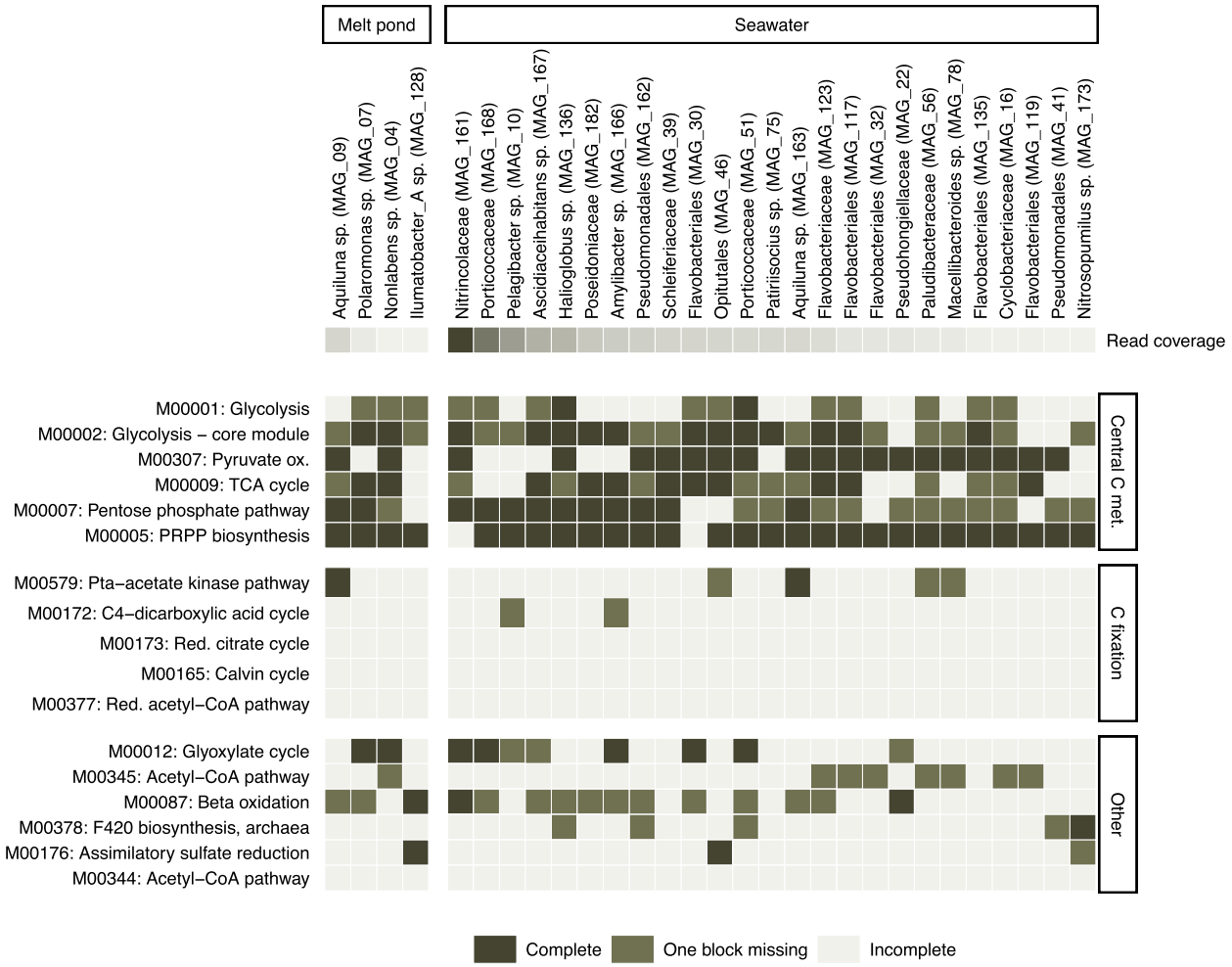

Fig. 3 Metabolic functions deduced from the MAGs. The MAGs were ordered based on abundance (read coverage) while showing the most abundant MAGs for both the melt pond ($n=4$) and the open water ($n=25$). The color code depicts the completeness of the KEGG modules, divided into three categories (complete, one block missing, and incomplete).

prokaryotic community based on MAGs is shown in Fig. S3a, b.

Relative abundance and clustering of viral OTUs

In total, 1154 dereplicated vOTUs were detected, of which 66.7% (770) were predicted to be phages. Of those, 79.6% and 20.4% were predicted to be virulent and temperate phages, respectively (Table S8). The > 5 µm and 0.2–5 µm filtered fractions of the melt pond SML were dominated by VC 960_0 (containing vOTU1148 and vOTU1151) corresponding to a Skunavirus-like family and shared protein similarities with marine Nonlabens phage P12024S (GenBank #JQ823122) [89] (Fig. 2b, Fig. S3c, Table S9) with 100% and 54.1% relative abundance, respectively. The melt pond ULW showed a prevalent vOTU identified as Singleton in vConTACT2 assigned to *Metaviridae* family and had 97.7 and 46.0% relative abundance on the > 5 µm and 0.2–5 µm pore-sized filters, respectively (Fig. 2b, Fig. S3c). Both SML and ULW contained the VC 429 and VC 430, which encompass vOTUs sharing protein similarities with the siphovirus Flavobacterium phage 11b (GenBank #AJ842011), previously isolated from Arctic sea-ice [14]. In total, only ten different vOTUs including the two very abundant vOTUs described above reached a relative abundance of > 2% in the melt pond, which shows that only a few viruses thrive there and adapt to the low diversity of hosts. In the open water, the alpha diversity was higher than in the melt pond (two-tailed Mann-Whitney *U*-test, *U* value = 0, $p=0.0040$, Fig. 2d), and vOTUs not assignable to known families were most abundant and found at every station (Fig. S3c). This was in line with the novelty of vOTUs as inferred from clustering proteins with viruses from a RefSeq database (Fig. 4, Table S9).

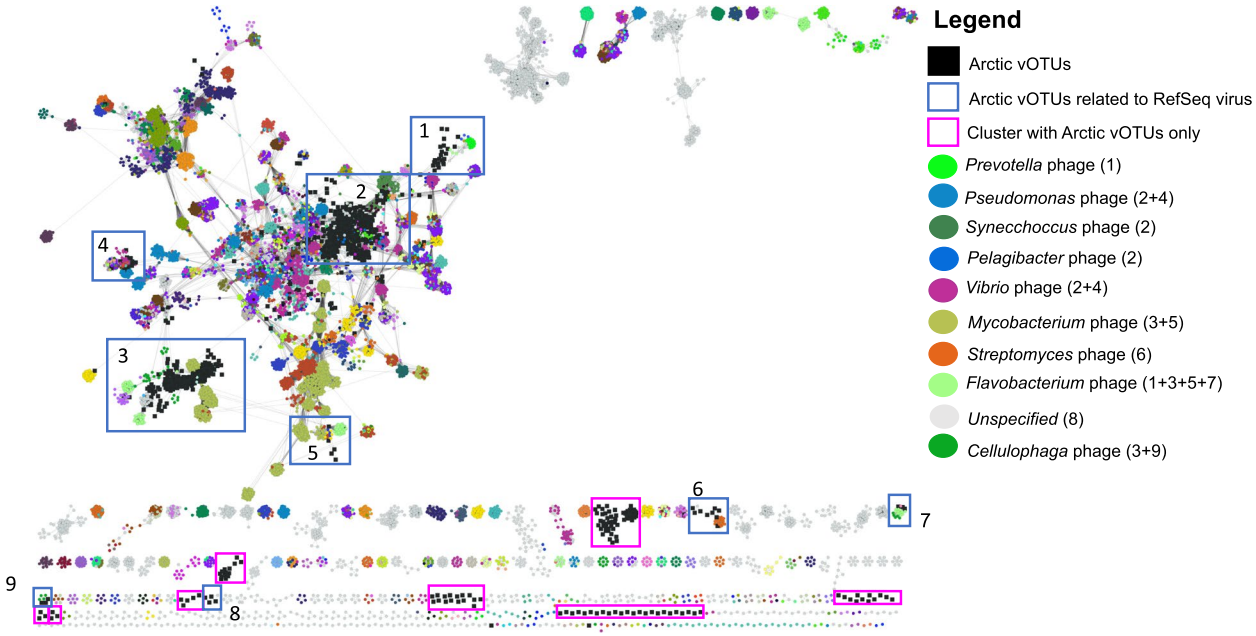

Fig. 4 Network of viral OTUs from this study clustered with viral genomes from the RefSeq database (July 2022) based on shared proteins. Blue, numbered frames show Arctic vOTUs clustering with known phages, with the most important clustering partners, including the host name, shown in the legend with frame number in parentheses. Pink frames indicate where Arctic vOTUs form clusters with each other

Host predictions and prophages in MAGs and isolate genomes

Host prediction using iPHoP could find 98 virus-host linkages at a minimum confidence score of 90 (Table S10, Fig. 5a), and of these, five vOTUs were predicted to have an archaeal host. The most common order of bacterial hosts was *Flavobacteriales*, to which 24 vOTUs were assigned. CRISPR analysis revealed that 8 of the 13 bacterial strains had CRISPR arrays as part of the adaptive immune system of prokaryotes. However, only one CRISPR spacer from the oceanic *Flavobacterium* sp. Arc2 matched a vOTU (coverage in melt pond = 214×) assembled from the melt pond virome (Table S11). This vOTU was also assigned to *Flavobacterium* as the host in iPHoP.

Prophages were mostly found in SML isolate genomes but were rare in MAGs (3 in bacteria, 2 in archaea, Table S4). Interestingly the archaeal MAGs 172 and 175 belonging to Marine Group II archaea within *Euryarchaeota* and sampled from Stations 42 and 50 both carried similar prophages. These had one auxiliary metabolic gene (AMGs) for glycine cleavage system H protein gcvH (KEGG database K02437) and glucose-1-phosphate thymidylyltransferase rfbA, rffH (KEGG database EC:2.7.7.24., K00973) involved in the biosynthesis of thymidine-linked sugars. In the remote Central Arctic, prophages might have an important function in assisting metabolic functions in these Archaea. Several prophages were found in bacterial isolate genomes from the SML, e.g., *Burkholderia vietnamiensis* Arc4 carried eight prophages, while *Bacillus pumilus* Arc15, *Psychrobacter* sp. Arc29, and *L. aequorea* Arc30 each carried two prophages, and *P. distincta* Arc38 and *Alcaligenes phenolicus* Arc10 (the latter likely being a contaminant associated with gangway sampling) both carried one prophage. All prophage annotations are reported in Table S4.

Auxiliary metabolic genes encoded by vOTUs

Using AnnoVIBRANT, we identified that 199 vOTUs (17.2% of all vOTUs) encoded for 87 unique AMGs (354 in total) with involvement in various, sometimes multiple metabolic pathways (Fig. 5b, Table S12). Of the AMG-carrying vOTUs, 26.6% carried more than one AMG and up to 12 in total (Fig. 5b, Table S13). Most abundant AMGs had predicted functions in amino acid metabolism (111), mainly in cysteine and methionine metabolism, in metabolism of cofactors and vitamins (118), mainly for porphyrin, as well as in glycan polymer and carbohydrate metabolism (both 71). AMGs related to cryoprotection of the host were also identified. Sixteen vOTUs carried the AMG glycerol-3-phosphate cytidylyltransferase or *tagD* [Enzyme Commission number, EC:2.7.7.39]. This gene encodes an enzyme involved in the production of teichoic acids [90], which in turn benefit freeze tolerance in bacteria [91, 92]. Three further AMGs were annotated as ice-binding-like [Pfam/InterPro database, PF11999.11],

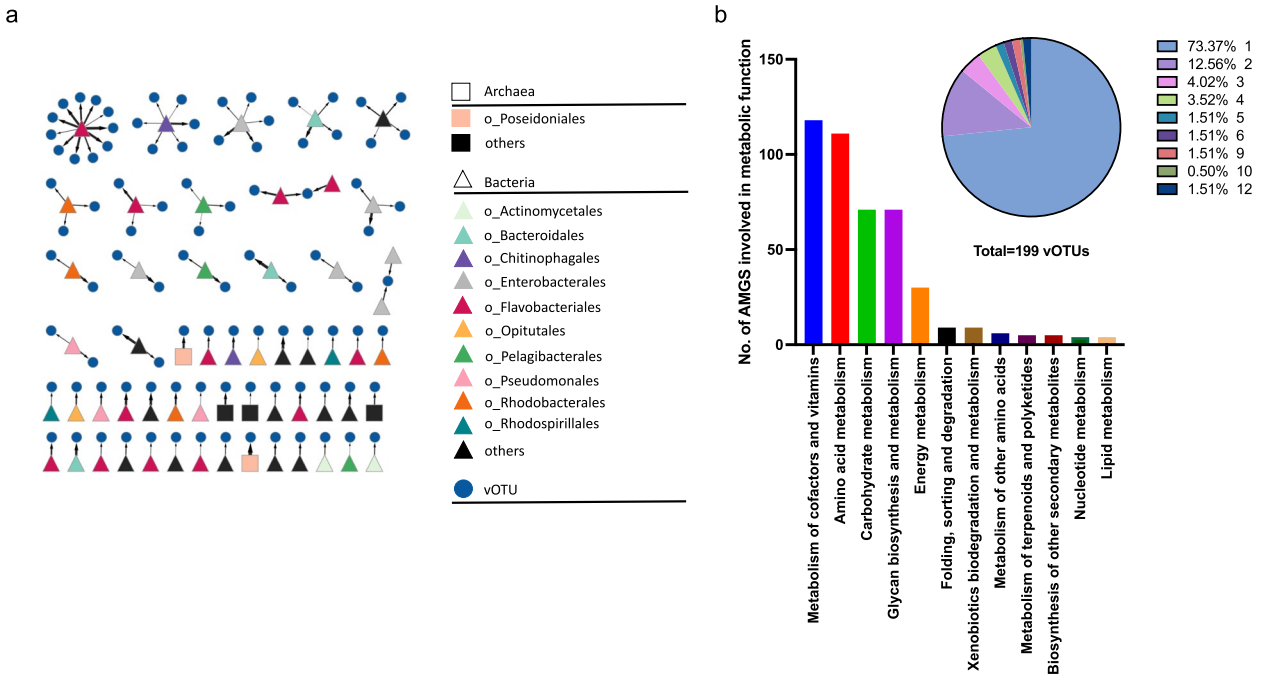

Fig. 5 Virus-host matches and auxiliary metabolic genes (AMGs). Host assignment for 96 Arctic vOTUs derived from iPHoP prediction (**a**). Minimum confidence score = 90; the thicker the arrow, the higher the confidence. For further details, please see Table S10. Number of AMGs involved in metabolic functions (**b**); 199 vOTUs carried 87 unique AMGs (354 in total) with involvements in different metabolic pathways (Table S12). The pie chart shows the percentage of vOTUs carrying one or more (up to 12) AMGs (Table S13)

which is a gene family that includes ice-binding proteins (IBPs). Screening Tara Oceans datasets for the presence and abundance of these two potential AMGs revealed that the homologs for *tagD* and the ice-binding like protein were detected at higher abundance in Northern and Southern Oceans (0.22–3 µm fraction) compared to regions around the equator (Figs. S4 and S5a). The highest abundances of these proteins mostly occurred at −1 to +3 °C in surface water. The abundances were even more strongly restricted to these regions in the transcriptomic compared to the metagenomic dataset (Figs. S4 and S5b). This indicates that the transcription of these genes correlates with low temperature, especially in surface water and the deep chlorophyll maximum. While homologs of the ice-binding-like protein were also associated with viruses, mostly Synechococcus phage S-SKS1, *tagD* only had bacterial homologs. Both sequences showed phylogenetic linkage to the order *Flavobacteriales*. In addition, vOTUs encoded genes related to cell wall metabolism were found, namely 199 AMGs for N-acetylmuramoyl-L-alanine amidase [EC:3.5.1.28], 140 AMGs for zinc D-Ala-D-Ala carboxypeptidase [EC:3.4.17.14], and 35 AMGs for peptidoglycan LD-endopeptidase CwlK [EC:3.4.-.-,]. All DRAM-v annotations of vOTUs are shown in Table S14.

Facilitated viral dispersal from the surface microlayer

By assuming that vOTU distribution through the Arctic would be mediated by the depth of the layer where the vOTU was found in (the closer to the atmosphere, the more prone to aerosolization, Fig. 6b), linear regressions were performed for vOTU abundance based on read coverage, and the number of stations a vOTU was present (based on read mapping). We found positive correlations for both vOTUs from SML and ULW, but a steeper slope for the SML (1.254) compared to the ULW (0.4673, Fig. 6a), indicating that vOTU abundance changes in the SML are more relevant for spreading to different stations than changes in the ULW. The goodness of fit was better for SML ($R^2 = 0.49$) than for ULW ($R^2 = 0.25$) data. Spearman r for the positive correlation between vOTU abundance and the number of stations where vOTUs were detected was 0.78 ($n = 375$) and 0.38 ($n = 649$) for SML and ULW, respectively. Statistics for group comparisons are shown in the supplement material (Fig. S6).

Prophage induction from strain *Leeuwenhoekiella aequorea* Arc30

The *L. aequorea* Arc30 culture showed a drop in OD_{600} ~ 4 h after addition of mitomycin C (1 and

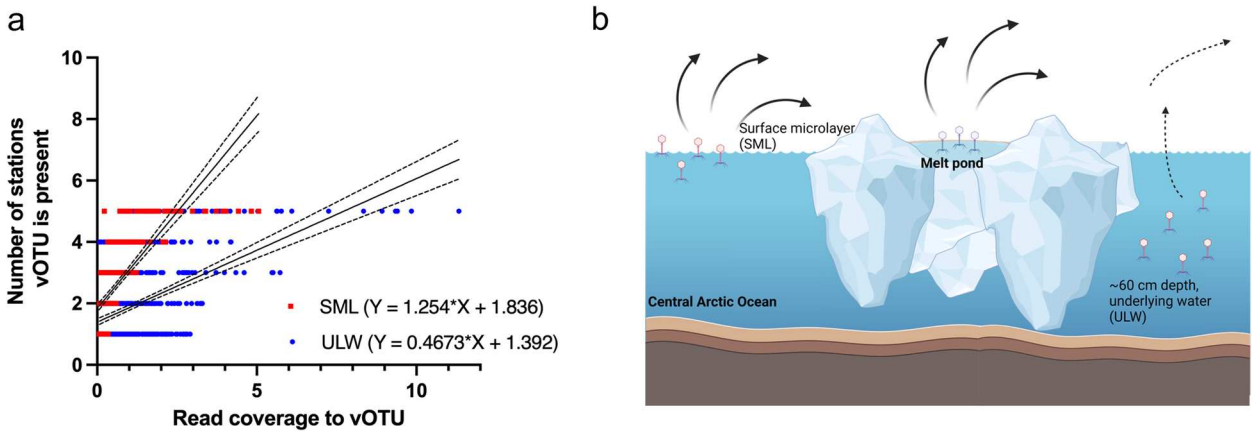

Fig. 6 Correlation of vOTUs coverage with presence at stations. Linear regressions (mean with confidence intervals) showing the positive correlation between the vOTU average read coverage for SML and ULW with the number of stations a vOTU was present based on read breadth (**a**). The concept figure illustrates the intensified spread of viruses from surface films of the Arctic Ocean and melt pond air-sea interface compared to deeper surface water irrespective of the higher abundance of phages in the ULW (**b**)

0.5 µg mL^{-1}) but not in the 0.1 µg mL^{-1} and no mitomycin C condition, and together with phage appearance in TEM, this indicated prophage induction to the lytic cycle (Fig. 7a). This OD drop was reproducible in several independent induction experiments. Within the genome of *L. aequorea* Arc30, VIBRANT predicted two prophages with genome lengths of 36.4 kb and 44.1 kb. Mapping of reads from the induction's supernatant to both prophage regions of the host showed that both prophage regions had a very high coverage, indicating induction and thus activity of both prophages (Fig. S7). Whole-genome sequencing of the phages from the supernatant after induction revealed that the 44.1 kb genome was circularizable (Fig. 7b), had a length of 42.7 kb, 34.91% GC content, and 75 open reading frames. Genes encoding structural proteins were found in above-average GC regions, while DNA replication/recombination/repair and packaging genes were found in below-average GC regions (Fig. 7b), a feature which might be relevant in extreme environments [93]. The integration site of the 44.1 kb prophage was a host tRNA for methionine (codon CAT), and the phage itself carries a tRNA for tryptophan (codon CCA).

Phylogenetic placement of new Arctic phages and database hits

For the induced 44.1 kb prophage (42.7 kb when excised), we propose the name Leeuwenhoekiella phage vB_LaeS_Arctus_1. Arctus_1 is distantly related to known *Polaribacter* phages based on shared proteins (Fig. 7d, Fig. S8), but the intergenomic similarity to these phages is < 1.3% (Fig. S9). We propose "Leeuwenvirus" and "Leeuwenvirus arctus" as new genus and species names for Arctus_1, respectively. As a viral family name, we propose *Neustonviridae* because the virus was isolated from the SML, where the neuston organisms reside.

The genome of the other, 36.4 kb prophage (35.4 kb when excised) was found in three independent assemblies, but the genome could not be circularized and thus might not be complete. This phage genome shares nine core proteins with Winogradskyella phage Peternella_1 (GenBank #NC_062754) isolated from the surface water of the North Sea [94] (Fig. S8). Hence, we suggest assigning it to the same family, *Winoviridae*. The phage genome has 42.0% GC content and 43 open reading frames. We propose the name Leeuwenhoekiella phage vB_LaeS_Arctica_1 and "Leeuwenhoekiellavirus" and "Leeuwenhoekiellavirus arctica" as new genus and species names for Arctica_1. Arctus_1 and Arctica_1 share 4.2% intergenomic similarity with each other (Fig. S9). Shared core proteins and functional annotations for the phages are shown in Table S15. The genomes of Arctus_1 and Arctica_1 had hits against genomes from uncultivated viruses assigned to the class *Caudoviricetes* in the IMG/VR database originating from marine, freshwater, and saltwater ecosystems from around the globe, including Arctic and Antarctic ecosystems, and additionally matched against genomes of other *Leeuwenhoekiella* sp. strains (Table S16). No evidence for cross-infection between supernatants with induced phage and *L. aequorea* strain CCUG 50091^{T} could be found for this phage-host pair in plaque assays or liquid culture.

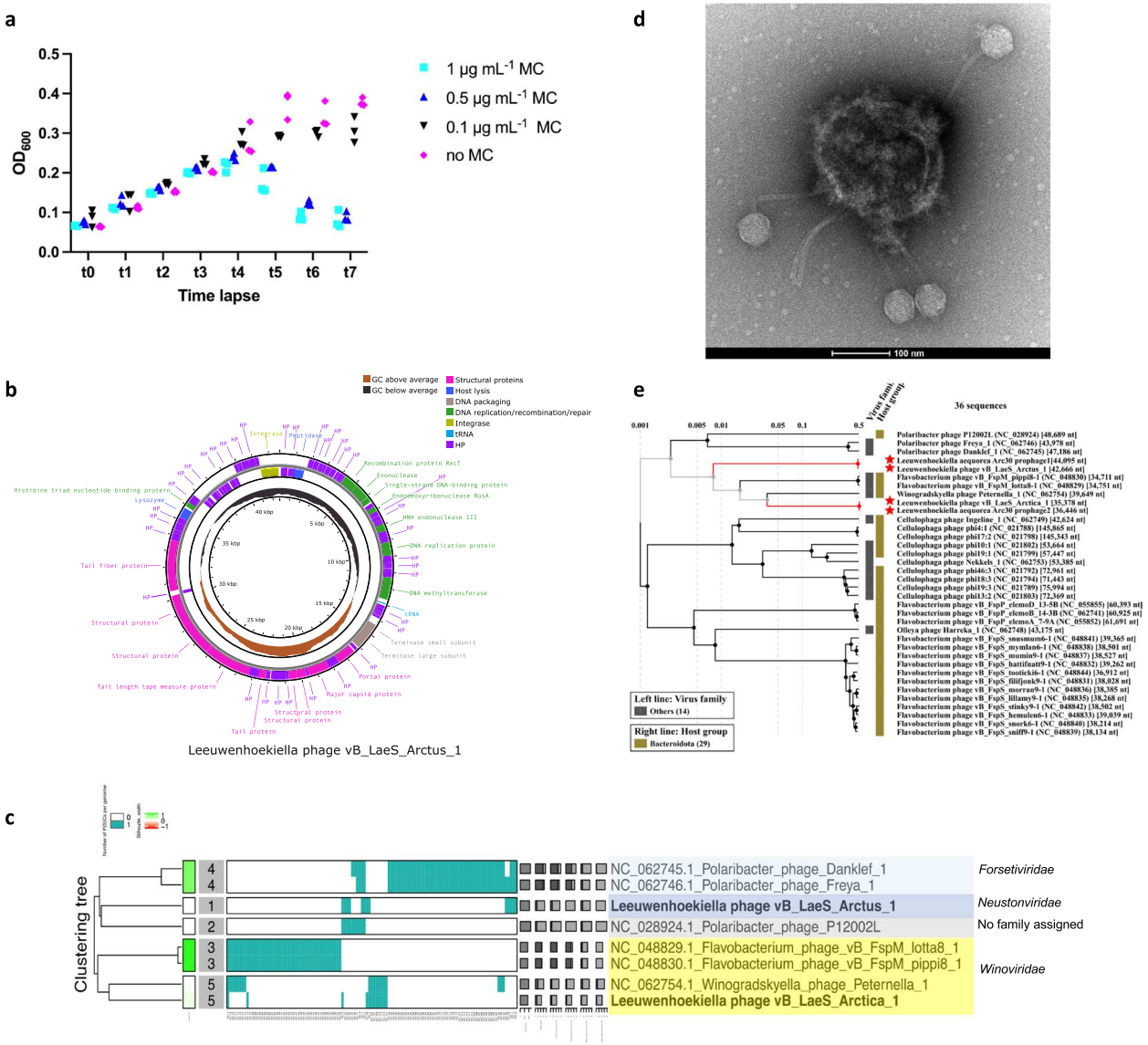

Fig. 7 Induction of two *Leeuwenhoekiella* prophages. Growth curve of the strain *Leeuwenhoekiella aequorea* Arc30 indicating prophage induction by mitomycin C treatment at t4 (**a**). The architecture of the 42.7 kb circular genome belonging to the induced Leeuwenhoekiella phage vB_LaeS_Arctus_1 (**b**). Protein clustering tree of Arctus_1 and Arctica_1 with related phages (**c**). TEM imaging at 68 k magnification revealed siphoviruses attached to a lysing host cell in the supernatant of the bacterium *L. aequorea* Arc30 after treatment with mitomycin C (**d**). A proteomic tree showing the placement of Leeuwenhoekiella phage vB_LaeS_Arctus_1 (**e**)

Morphology of induced phages

TEM imaging revealed siphoviruses (head and non-contractile tail) in the supernatant of induced *L. aequorea* Arc30 lysogen, with the phages attached to the lysed host cell (Fig. 7c). The phages had a mean ± standard deviation diameter of the capsid of 50.4 ± 3.0 nm ($n = 24$) and a tail length of 157.7 ± 12.2 nm ($n = 16$, Table S17). Arctus_1 had a tape measure protein of 978 amino acids in length (for sequence see Supplement material). According to a formula proposed earlier [95], the calculated tail length of that phage would be 154.8 nm, which is very close to the length of the phage observed in TEM. Arctica_1 had no identifiable tape measure protein.

Discussion

The aim of this study was to investigate viral-bacterial interactions in atmosphere-close aquatic ecosystems of the Central Arctic. Our study shows that viral and bacterial diversity were lower in the melt pond compared to the oceanic samples. Melt ponds form due to melting

sea ice and snow in the Arctic summer and are typically not connected with the ocean underneath the ice. Due to their shallow depth, melt pond water is prone to more freeze-thaw cycles, with the lowest temperature at the surface of the pond (where the SML exists) [96]. This adds an extra burden to the organisms and viruses living there and probably restricts their diversity. A lower alpha diversity as well as a different community composition of microbial eukaryotes in melt ponds compared to seawater has been previously reported [97]. We noticed that only two melt pond viruses became very abundant in filtered fractions > 0.2 µm suggesting that they responded to and thrived well on the few available hosts. Melt ponds select for *Flavobacteria* (*Bacteroidota*), *Betaproteobacteria*, and *Alphaproteobacteria* depending on factors such as whether melt ponds are open or closed as well as the salinity of the water [98, 99]. The melt pond studied here was open when sampled and primarily enriched in *Pseudomonadota* such as *Polaromonas* sp. (MAG_01), *Bacteroidota* such as *Flavobacterium* sp. (Arc3) and *Nonlabens* sp. (MAG_04), as well as *Actinomycetota* such as *Aquiluna* sp. (MAG_03). Due to their disconnection from the ocean, the major source for biological input, including viruses, into melt ponds is probably melting ice and atmospheric exchange. Sea ice algae, such as the diatom *Melosira arctica*, which was observed during this cruise, can form large aggregates in melt ponds (reviewed by [100]). The SML from the sampled melt pond was highly viscous (personal observation), suggesting that algae-derived extracellular polymeric substances (EPS) were likely present. This would also explain the predominance of the family *Metaviridae*, which includes retrotransposons and reverse-transcribing viruses targeting eukaryotes [101] and thus potentially algae. However, while we provide first insights into viruses from melt ponds, a clear limitation of our study is that only a single melt pond could be sampled. This leads to the question of whether different melt ponds contain similar or different viral-bacterial communities, which must be addressed in future investigations. Studying viruses in melt ponds in summer could help to elucidate the effects of solar and UV radiation while investigating viruses from frozen melt ponds that receive very little light could be worthwhile in winter.

Virus-encoded AMGs related to cryosurvival have previously been described for viruses from the Southern Ocean [102], including genes related to cell wall polymer and EPS production, as well as cold shock genes. The latter have also been detected in viruses from Arctic glacial ice [103]. IBPs have been described in many bacteria [104, 105], where they prevent damage from ice crystals by binding to ice surfaces and inhibiting their growth. An antifreeze protein belonging to a subset of the IBPs has been found in viruses derived from metagenomes of the Southern Ocean [102]. In addition to IBPs, we also found AMGs encoding for glycerol-3-phosphate cytidylyltransferase, which has a function in the biosynthesis of teichoic acid, a cell wall component of Gram-positive bacteria. Constituents of teichoic acids undergo chemical interactions that allow liquid water to be maintained within the cell wall and the immediate extracellular space [91, 92] thereby providing cryoprotection. Teichoic acids can also be secreted into extracellular spaces, for instance within biofilms [106]. Possessing these AMGs, which seem to be widespread in the Northern and Southern Oceans, might increase the chances of host viability around 0 ℃ and thus benefit viral replication and dissemination under harsh conditions. Having antifreeze and freeze-tolerance genes in the SML can represent a meaningful advantage, namely that the bacterial hosts acquire cryoprotection in habitats exposed to freezing. When sea water freezes, the formation of ice typically initiates at the surface due to direct exposure to cold air, gradually expanding downward as the freezing process continues.

We noticed that vOTU distribution to many stations was more strongly positively correlated with average coverage for SML vOTUs than for ULW vOTUs, despite the average coverage of a vOTU overall being higher in ULW. An explanation could be that viral accumulation in SML facilitates their aerosolization and atmospheric distribution, allowing viruses to spread more easily through the Arctic. It follows that aerosolization might be easier for low- to medium-abundant vOTUs in the SML than for higher-abundant ones in the ULW. Whether such a correlation exists for other oceans, however, remains to be understood. The aerosolization of viruses from SML is a known feature [15, 16, 107] and is heavily mediated by bubbles that rise to the surface and scavenge viruses [108, 109]. Recent work with tank experiments has shown that virus transfer leading to aerosolization from water surfaces is related to the size of bubbles (the smaller, the more viruses) and their originating depth (the deeper, the more viruses are scavenged on the way to the surface) [110].

We found two inducible, i.e., active prophages for the low-abundant Arctic SML strain *L. aequorea* Arc30. In contrast, results from Baltic Sea SML showed that an inducible phage occurred in one of the most abundant bacterial strains, *Alishewanella* sp., which was also hunted by lytic phages [111]. *Flavobacteria*, which have previously been identified in the surface microlayer (SML) of various oceans as common hosts for both lytic and temperate phages [111–113], were also identified as significant predicted viral hosts in the Arctic in this study. Lysogeny is often prevalent or dominant in polar environments [79, 114, 115]. A switch from lysogenic to

lytic viral lifestyle mainly happens when bacterial production increases as shown for samples from the Southern Ocean [114]. However, even in environments of low productivity, viruses can be active and infect key prokaryotes as shown by a recent study on virioplankton from under the Antarctic Ross Ice Shelf [116]. Similarly, in a previous investigation on virioneuston activity from the Arctic and Antarctica, the lytic viral strategy dominated over lysogeny as deduced from calculations on flow cytometry counts of virus-like particles and prokaryotes after mitomycin C treatment of water samples [22], matching our observation of (inducible) prophages in the Central Arctic's SML. How often prophage inductions happen spontaneously in nature is another question that warrants further investigation. The SML, compared to the pelagic ocean, may be a more virally active ecosystem in the Arctic, particularly in summer, when long hours of solar and UV radiation hit the air-sea boundary and naturally enhance phage induction [117]. This might be counter-balanced by salinity effects as high, but not low, salinity was associated with higher titers of the marine phage varphiHSIC infecting *Listonella pelagia*, and elevated salinity could influence the switch from lysogenic to lytic cycle [118]. Melting sea ice results in a less saline SML, therefore potentially favoring lysogeny. As the samples were retrieved close to ice edges (Fig. 1b), this could explain the many SML-associated (compared to ULW) prophages detected in this study. The salinity of the surface microlayer (SML) is subject to fluctuations [119]. It responds immediately to freshwater inputs, such as rainwater [120], but can become more saline than the ULW due to evaporation effects [121]. Like in any other ocean [122], the SML in polar regions is usually colder than the ULW, which is known as the cool skin layer effect [123]. We thus speculate that the lifestyle of the Arctic virioneuston, in contrast to the virioplankton, is under a stronger pressure to adapt to the cold temperature and freezing/melting ice conditions in an environment with limited host diversity.

Conclusions

In conclusion, our data sheds light on virus-host interactions in aquatic ecosystems of the Central Arctic Ocean, specifically in the aquatic environment interfacing with the atmosphere. The melt pond viral community differed from the oceanic viruses and responded to the availability of a few hosts. *Flavobacteria* play a crucial role as viral hosts in both aquatic environments; however, their diversity is more pronounced in the ocean. All prophages (except for one) were found in MAGs or isolate genomes derived from the SML, and for the bacterial strain *L. aequorea* Arc30, we demonstrated the prophage's activity. Lysogeny might prevail in the SML at times when influences of melting ice make the SML less saline. From the SML, vOTUs are more easily distributed across the Arctic, and some vOTUs from the first centimeters of the water surface potentially contribute to the freezing tolerance of their hosts by carrying relevant AMGs. We conclude that in the Central Arctic, viruses have developed sophisticated strategies for adapting to challenging conditions. Despite the anticipated increase in ice loss and significant perturbations in the coming decades, it appears that viruses are well-equipped to persist and thrive in this ecosystem.

Abbreviations

AMG	Auxiliary metabolic gene
CRISPR	Clustered regularly interspaced short palindromic repeat
EPS	Extracellular polymeric substances
IBP	Ice-binding protein
iRep	Index of Replication
KEGG	Kyoto Encyclopedia of Genes and Genomes
MAG	Metagenome-assembled genome
SML	Surface microlayer
ULW	Underlying surface water
TEM	Transmission electron microscopy
vOTU	Viral operational taxonomic unit

Supplementary Information

The online version contains supplementary material available at https://doi.org/10.1186/s40168-024-01902-0.

Additional file 1. A .docx file with seven additional figures and more text information.

Additional file 2. A .xlsx file including 18 tables. The titles of the tables are TableS1_Sampling_info (Table S1), TableS2_MAG_breadth (Table S2), TableS3_Bacterial_isolates (Table S3), TableS4_Prophages (Table S4), TableS5_results_motus (Table S5), TableS6_MAGs (Table S6), TableS7_iRep (Table S7), TableS8_PhaMer_Phatyp (Table S8), TableS9_vOTU_VCinfo (Table S9), TableS10_Host_prediction (Table S10), TableS11_CRISPRmatches (Table S11), TableS12_AMGnumbers (Table S12), TableS13_AMGonvOTU (Table S13), TableS14_vOTU_annotations (Table S14), TableS15_Phage_Annotations (Table S15), TableS16_TEM measure (Table S16), TableS17_IMGVR hits (Table S17), TableS18_Bioproject_PRJNA950101 (Table S18).

Acknowledgements

The Swedish Polar Research Secretariat (SPRS; https://polar.se) organized and supported the SAS-Oden 2021 expedition with IB Oden in the Central Arctic Ocean. This expedition was the Swedish contribution to the International "Synoptic Arctic Survey" (SAS; https://synopticarcticsurvey.w.uib.no/). We thank the Master and crew of IB Oden for expertly undertaking the SAS-Oden 2021 expedition. We particularly thank the chief scientist Pauline Snoeijs Leijonmalm and Maria Samuelsson for enabling and supporting the project. We further acknowledge help by the science party, and in particularly Claudia Morys, Emma Svahn, Julia Muchowski, Sonja Murto, and John Prytherch for assistance during SML sampling. We thank Maria Chechik for help with TEM imaging. We thank Leonie Jaeger for discussions on the cool-skin layer effect. We acknowledge support from the National Genomics Infrastructure in Stockholm funded by Science for Life Laboratory, the Knut and Alice Wallenberg Foundation and the Swedish Research Council for assistance with massively parallel sequencing and access to the UPPMAX computational infrastructure. Data handling was enabled by resources provided by the National Academic Infrastructure for Supercomputing in Sweden (NAISS) and the Swedish National Infrastructure for Computing (SNIC2020-16-49) at UPPMAX partially funded by the Swedish Research Council through grant agreement no. 2022-06725 and no. 2018-05973. We like to thank Pavlin Mitev at UPPMAX for support.

Authors' contributions
JR conducted sampling, experimental work, data analysis, and wrote the first draft of the manuscript, and together with KH isolated bacteria, contributed to prophage analysis and provided funding for this work. GW conducted metabolic analysis on MAGs and provided community plots. JW contributed to prophage induction experiments. AA provided TEM images of the induced phage. All authors contributed to editing and writing of the manuscript.

Funding
Open access funding provided by Linnaeus University. JR was funded by the projects "Exploring the virioneuston: Viral-bacterial interactions between ocean and atmosphere (VIBOCAT)" by the German Research Foundation (DFG RA3432/1-1, project number: 446702140) and the DFG Walter-Benjamin Return Grant (RA3432/1-3, project number 534276621). KH and JR received funding from the Swedish Research Council, nr 2022-04340 and 2023-03310_VR, respectively. JW was supported by Carl Tryggers Foundation grant number CTS20:128. AA was funded by the Wellcome Trust investigator award 224665.

Data availability
The sequencing datasets supporting the conclusions of this article are available at NCBI's Sequence Read Archive under Bioproject ID PRJNA950101, Biosample accessions SAMN33983821 – SAMN33973845. Bacterial isolate genomes are stored at GenBank under Biosample accessions SAMN35056136 – SAMN35056148. The 182 MAGs are stored under Biosample accessions SAMN34587563 – SAMN34587744. The vOTUs are stored under Biosample SAMN33983825. The genomes of Arctus_1 and Arctica_1 can be found under GenBank accessions PP314354 and PP476357. For further information (e.g. run accessions) please see Table S18. TEM images are available at Figshare, doi: https://doi.org/10.6084/m9.figshare.25343113.

Declarations

Ethics approval and consent to participate
Not applicable to the present study.

Consent for publication
Maria Chechik, University of York, provided consent to publish her TEM images.

Competing interests
The authors declare no competing interests.

Author details
[1]Centre for Ecology and Evolution in Microbial Model Systems (EEMiS), Department of Biology and Environmental Science, Linnaeus University, Kalmar, Sweden. [2]Aero-Aquatic Virus Research Group, Faculty of Mathematics and Computer Science, Friedrich Schiller University Jena, Jena, Germany. [3]Leibniz Institute on Aging-Fritz Lipmann Institute (FLI), Jena, Germany. [4]York Structural Biology Laboratory, Department of Chemistry, University of York, York, UK.

Received: 18 March 2024 Accepted: 6 August 2024
Published online: 24 October 2024

References

1. Lannuzel D, Tedesco L, van Leeuwe M, Campbell K, Flores H, Delille B, et al. The future of Arctic sea-ice biogeochemistry and ice-associated ecosystems. Nat Clim Change. 2020;10(11):983–92.
2. Landrum L, Holland MM. Extremes become routine in an emerging new Arctic. Nat Clim Change. 2020;10(12):1108–15.
3. Arrigo KR, van Dijken G, Pabi S. Impact of a shrinking Arctic ice cover on marine primary production. Geophys Res Lett. 2008;35(19).
4. Lavoie D, Denman KL, Macdonald RW. Effects of future climate change on primary productivity and export fluxes in the Beaufort Sea. J Geophys Res-Oceans. 2010;115(C4).
5. Suttle CA. Marine viruses–major players in the global ecosystem. Nat Rev Microbiol. 2007;5(10):801–12.
6. Weinbauer MG, Rassoulzadegan F. Are viruses driving microbial diversification and diversity? Environ Microbiol. 2004;6(1):1–11.
7. Heinrichs ME, et al. Breaking the Ice: A Review of Phages in Polar Ecosystems. In: Tumban, E. (eds) Bacteriophages. Methods in Molecular Biology, vol 2738. New York: Humana; 2024. https://doi.org/10.1007/978-1-0716-3549-0_3.
8. Engel A, Bange HW, Cunliffe M, Burrows SM, Friedrichs G, Galgani L, et al. The ocean's vital skin: toward an integrated understanding of the sea surface microlayer. Front Mar Sci. 2017;4:165.
9. Hardy JT. The sea surface microlayer: biology, chemistry and anthropogenic enrichment. Prog Oceanogr. 1982;11(4):307–28.
10. Deming JW, Eric Collins R. Sea ice as a habitat for Bacteria, Archaea and viruses. In: Thomas DN, editor. Sea ice. 2016. p. 326–51.
11. Galgani L, Piontek J, Engel A. Biopolymers form a gelatinous microlayer at the air-sea interface when Arctic sea ice melts. Sci Rep. 2016;6(1):29465.
12. Webster MA, Rigor IG, Perovich DK, Richter-Menge JA, Polashenski CM, Light B. Seasonal evolution of melt ponds on Arctic sea ice. J Geophys Res-Oceans. 2015;120(9):5968–82.
13. Borriss M, Helmke E, Hanschke R, Schweder T. Isolation and characterization of marine psychrophilic phage-host systems from Arctic sea ice. Extremophiles. 2003;7(5):377–84.
14. Borriss M, Lombardot T, Glockner FO, Becher D, Albrecht D, Schweder T. Genome and proteome characterization of the psychrophilic *Flavobacterium* bacteriophage 11b. Extremophiles. 2007;11(1):95–104.
15. Aller JY, Kuznetsova MR, Jahns CJ, Kemp PF. The sea surface microlayer as a source of viral and bacterial enrichment in marine aerosols. J Aerosol Sci. 2005;36(5–6):801–12.
16. Rahlff J, Esser SP, Plewka J, Heinrichs ME, Soares A, Scarchilli C, et al. Marine viruses disperse bidirectionally along the natural water cycle. Nat Commun. 2023;14(1):6354.
17. Wagner R, Ickes L, Bertram AK, Els N, Gorokhova E, Möhler O, et al. Heterogeneous ice nucleation ability of aerosol particles generated from Arctic sea surface microlayer and surface seawater samples at cirrus temperatures. Atmos Chem Phys. 2021;21(18):13903–30.
18. Wilson TW, Ladino LA, Alpert PA, Breckels MN, Brooks IM, Browse J, et al. A marine biogenic source of atmospheric ice-nucleating particles. Nature. 2015;525(7568):234–8.
19. Adams MP, Atanasova NS, Sofieva S, Ravantti J, Heikkinen A, Brasseur Z, et al. Ice nucleation by viruses and their potential for cloud glaciation. Biogeosciences. 2021;18(14):4431–44.
20. Gregory AC, Zayed AA, Conceicao-Neto N, Temperton B, Bolduc B, Alberti A, et al. Marine DNA viral macro- and microdiversity from pole to pole. Cell. 2019;177(5):1109-23.e14.
21. Rahlff J. The virioneuston: a review on viral(-)bacterial associations at air(-)water interfaces. Viruses. 2019;11(2):191.
22. Vaqué D, Boras JA, Arrieta JM, Agusti S, Duarte CM, Sala MM. Enhanced viral activity in the surface microlayer of the Arctic and Antarctic Oceans. Microorganisms. 2021;9(2):317.
23. Sazhin AF, Romanova N, Kopylov A, Zabotkina E. Bacteria and viruses in Arctic sea ice. Oceanology. 2019;59(3):339–46.
24. Dahlbäck B, Gunnarsson LÅH, Hermansson M, Kjelleberg S. Microbial investigations of surface microlayers, water column, ice and sediment in the Arctic Ocean. Mar Ecol Progr Ser. 1982;9(1):101–9.
25. Vaqué D, Lara E, Arrieta JM, Holding J, Sa EL, Hendriks IE, et al. Warming and CO_2 enhance Arctic heterotrophic microbial activity. Front Microbiol. 2019;10:494.
26. Gao C, Xia J, Zhou X, Liang Y, Jiang Y, Wang M, et al. Viral characteristics of the warm Atlantic and cold Arctic water masses in the Nordic Seas. Appl Environ Microbiol. 2021;87(22):e0116021.
27. Snoeijs-Leijonmalm P. Expedition Report SWEDARCTIC Synoptic Arctic Survey 2021 with icebreaker Oden. Luleå: Swedish Polar Research Secretariat; 2022. p. 300.
28. Harvey GW, Burzell LA. A simple microlayer method for small samples. Limnol Oceanogr. 1972;17(1):156–7.
29. Ram ASP, Mari X, Brune J, Torreton JP, Chu VT, Raimbault P, et al. Bacterial-viral interactions in the sea surface microlayer of a black carbon-dominated tropical coastal ecosystem (Halong Bay, Vietnam). Elementa-Sci Anthrop. 2018;6(1):13.
30. Agogué H, Casamayor EO, Joux F, Obernosterer I, Dupuy C, Lantoine F, et al. Comparison of samplers for the biological characterization of the sea surface microlayer. Limnol Oceanogr-Meth. 2004;2(7):213–25.
31. Schlitzer R. Ocean Data View. 2022. https://odv.awi.de/.

32. John SG, Mendez CB, Deng L, Poulos B, Kauffman AK, Kern S, et al. A simple and efficient method for concentration of ocean viruses by chemical flocculation. Environ Microbiol Rep. 2011;3(2):195–202.
33. Langenfeld K, Chin K, Roy A, Wigginton K, Duhaime MB. Comparison of ultrafiltration and iron chloride flocculation in the preparation of aquatic viromes from contrasting sample types. PeerJ. 2021;9:e11111.
34. Bushnell B. BBTools software package. 2014;578:579. http://sourceforge.net/projects/bbmap.
35. Joshi N, Fass J. Sickle: a sliding-window, adaptive, quality-based trimming tool for FastQ files (version 1.33)[Software]. 2011.
36. Ruscheweyh HJ, Milanese A, Paoli L, Karcher N, Clayssen Q, Keller MI, et al. Cultivation-independent genomes greatly expand taxonomic-profiling capabilities of mOTUs across various environments. Microbiome. 2022;10(1):212.
37. Milanese A, Mende DR, Paoli L, Salazar G, Ruscheweyh HJ, Cuenca M, et al. Microbial abundance, activity and population genomic profiling with mOTUs2. Nat Commun. 2019;10(1):1014.
38. Team RC. R: a language and environment for statistical computing. Vienna: R Foundation for Statistical Computing; 2017.
39. McMurdie PJ, Holmes S. phyloseq: an R package for reproducible interactive analysis and graphics of microbiome census data. PLoS One. 2013;8(4):e61217.
40. Wickham H, Chang W, Wickham MH. Package 'ggplot2'. Create elegant data visualisations using the grammar of graphics Version. 2016;2(1):1–189.
41. Alneberg J, Bjarnason BS, de Bruijn I, Schirmer M, Quick J, Ijaz UZ, et al. Binning metagenomic contigs by coverage and composition. Nat Methods. 2014;11(11):1144–6.
42. Kang DD, Li F, Kirton E, Thomas A, Egan R, An H, Wang Z. MetaBAT 2: an adaptive binning algorithm for robust and efficient genome reconstruction from metagenome assemblies. PeerJ. 2019;7:e7359.
43. Nurk S, Meleshko D, Korobeynikov A, Pevzner PA. metaSPAdes: a new versatile metagenomic assembler. Genome Res. 2017;27(5):824–34.
44. Sieber CMK, Probst AJ, Sharrar A, Thomas BC, Hess M, Tringe SG, Banfield JF. Recovery of genomes from metagenomes via a dereplication, aggregation and scoring strategy. Nat Microbiol. 2018;3(7):836–43.
45. Bornemann TLV, Esser SP, Stach TL, Burg T, Probst AJ. uBin: a manual refining tool for genomes from metagenomes. Environ Microbiol. 2023;25(6):1077–83.
46. Chklovski A, Parks DH, Woodcroft BJ, Tyson GW. CheckM2: a rapid, scalable and accurate tool for assessing microbial genome quality using machine learning. Nat Methods. 2023;20(8):1203–12.
47. Parks DH, Imelfort M, Skennerton CT, Hugenholtz P, Tyson GW. CheckM: assessing the quality of microbial genomes recovered from isolates, single cells, and metagenomes. Genome Res. 2015;25(7):1043–55.
48. Chaumeil PA, Mussig AJ, Hugenholtz P, Parks DH. GTDB-Tk v2: memory friendly classification with the genome taxonomy database. Bioinformatics. 2022;38(23):5315–6.
49. Olm MR, Brown CT, Brooks B, Banfield JF. dRep: a tool for fast and accurate genomic comparisons that enables improved genome recovery from metagenomes through de-replication. ISME J. 2017;11(12):2864–8.
50. Brown CT, Olm MR, Thomas BC, Banfield JF. Measurement of bacterial replication rates in microbial communities. Nat Biotechnol. 2016;34(12):1256–63.
51. Cantalapiedra CP, Hernández-Plaza A, Letunic I, Bork P, Huerta-Cepas J. eggNOG-mapper v2: functional annotation, orthology assignments, and domain prediction at the metagenomic scale. Mol Biol Evol. 2021;38(12):5825–9.
52. Antipov D, Raiko M, Lapidus A, Pevzner PA. Metaviral SPAdes: assembly of viruses from metagenomic data. Bioinformatics. 2020;36(14):4126–9.
53. Kieft K, Zhou Z, Anantharaman K. VIBRANT: automated recovery, annotation and curation of microbial viruses, and evaluation of viral community function from genomic sequences. Microbiome. 2020;8(1):90.
54. Guo J, Bolduc B, Zayed AA, Varsani A, Dominguez-Huerta G, Delmont TO, et al. VirSorter2: a multi-classifier, expert-guided approach to detect diverse DNA and RNA viruses. Microbiome. 2021;9(1):37.
55. Nayfach S, Camargo AP, Schulz F, et al. CheckV assesses the quality and completeness of metagenome-assembled viral genomes. Nat Biotechnol. 2020;39:578–85.
56. Moraru C, Varsani A, Kropinski AM. VIRIDIC-a novel tool to calculate the intergenomic similarities of prokaryote-infecting viruses. Viruses. 2020;12(11):1268.
57. Nilsson E, Bayfield OW, Lundin D, Antson AA, Holmfeldt K. Diversity and host interactions among virulent and temperate Baltic Sea *Flavobacterium* phages. Viruses. 2020;12(2):158.
58. Roux S, Emerson JB, Eloe-Fadrosh EA, Sullivan MB. Benchmarking viromics: an in silico evaluation of metagenome-enabled estimates of viral community composition and diversity. PeerJ. 2017;5:e3817.
59. Rahlff J, Bornemann TLV, Lopatina A, Severinov K, Probst AJ. Host-associated phages disperse across the extraterrestrial analogue Antarctica. Appl Environ Microbiol. 2022;88(10):e0031522.
60. Shang J, Peng C, Liao H, Tang X, Sun Y. PhaBOX: a web server for identifying and characterizing phage contigs in metagenomic data. Bioinform Adv. 2023;3(1):vbad101.
61. Shang J, Tang X, Guo R, Sun Y. Accurate identification of bacteriophages from metagenomic data using Transformer. Brief Bioinform. 2022;23(4):bbac258.
62. Shang J, Tang X, Sun Y. PhaTYP: predicting the lifestyle for bacteriophages using BERT. Brief Bioinform. 2023;24(1):bbac487.
63. Bolduc B, Jang HB, Doulcier G, You ZQ, Roux S, Sullivan MB. vConTACT: an iVirus tool to classify double-stranded DNA viruses that infect Archaea and Bacteria. PeerJ. 2017;5:e3243.
64. Cook R, Brown N, Redgwell T, Rihtman B, Barnes M, Clokie M, et al. Infrastructure for a phage reference database: identification of large-scale biases in the current collection of cultured phage genomes. Phage. 2021;2(4):214–23.
65. Pandolfo M, Telatin A, Lazzari G, Adriaenssens EM, Vitulo N. MetaPhage: an automated pipeline for analyzing, annotating, and classifying bacteriophages in metagenomics sequencing data. mSystems. 2022;7(5):e0074122.
66. Shang J, Jiang J, Sun Y. Bacteriophage classification for assembled contigs using graph convolutional network. Bioinformatics. 2021;37(Suppl_1):i25–33.
67. Jiang JZ, Yuan WG, Shang J, Shi YH, Yang LL, Liu M, et al. Virus classification for viral genomic fragments using PhaGCN2. Brief Bioinform. 2023;24(1):bbac505.
68. Hurwitz BL, U'Ren JM. Viral metabolic reprogramming in marine ecosystems. Curr Opin Microbiol. 2016;31:161–8.
69. Hyatt D, Chen GL, Locascio PF, Land ML, Larimer FW, Hauser LJ. Prodigal: prokaryotic gene recognition and translation initiation site identification. BMC Bioinformatics. 2010;11(1):119.
70. Shaffer M, Borton MA, McGivern BB, Zayed AA, La Rosa SL, Solden LM, et al. DRAM for distilling microbial metabolism to automate the curation of microbiome function. Nucleic Acids Res. 2020;48(16):8883–900.
71. Vernette C, Lecubin J, Sanchez P, Tara Oceans C, Sunagawa S, Delmont TO, et al. The Ocean Gene Atlas v2.0: online exploration of the biogeography and phylogeny of plankton genes. Nucleic Acids Res. 2022;50(W1):W516–26.
72. Villar E, Vannier T, Vernette C, Lescot M, Cuenca M, Alexandre A, et al. The Ocean Gene Atlas: exploring the biogeography of plankton genes online. Nucleic Acids Res. 2018;46(W1):W289–95.
73. Roux S, Camargo AP, Coutinho FH, Dabdoub SM, Dutilh BE, Nayfach S, Tritt A. iPHoP: an integrated machine learning framework to maximize host prediction for metagenome-derived viruses of archaea and bacteria. PLoS Biol. 2023;21(4):e3002083.
74. Shannon P, Markiel A, Ozier O, Baliga NS, Wang JT, Ramage D, et al. Cytoscape: a software environment for integrated models of biomolecular interaction networks. Genome Res. 2003;13(11):2498–504.
75. Fridolfsson E, Bunse C, Lindehoff E, Farnelid H, Pontiller B, Bergstrom K, et al. Multiyear analysis uncovers coordinated seasonality in stocks and composition of the planktonic food web in the Baltic Sea proper. Sci Rep. 2023;13(1):11865.
76. Couvin D, Bernheim A, Toffano-Nioche C, Touchon M, Michalik J, Neron B, et al. CRISPRCasFinder, an update of CRISRFinder, includes a portable version, enhanced performance and integrates search for Cas proteins. Nucleic Acids Res. 2018;46(W1):W246–51.
77. Levine M. Effect of mitomycin C on interactions between temperate phages and bacteria. Virology. 1961;13(4):493–9.
78. Nilsson E, Li K, Fridlund J, Sulcius S, Bunse C, Karlsson CMG, et al. Genomic and seasonal variations among aquatic phages infecting the Baltic Sea *Gammaproteobacterium Rheinheimera* sp. Strain BAL341. Appl Environ Microb. 2019;85(18):e01003-19.
79. Liu Z, Jiang W, Kim C, Peng X, Fan C, Wu Y, et al. A *Pseudomonas* lysogenic bacteriophage crossing the Antarctic and Arctic, representing a new genus of *Autographiviridae*. Int J Mol Sci. 2023;24(8):7662.

80. Nedashkovskaya OI, Vancanneyt M, Dawyndt P, Engelbeen K, Vandemeulebroecke K, Cleenwerck I, et al. Reclassification of *[Cytophaga] marinoflava* Reichenbach 1989 as *Leeuwenhoekiella marinoflava* gen. nov., comb. nov. and description of *Leeuwenhoekiella aequorea* sp. nov. Int J Syst Evol Microbiol. 2005;55(Pt 3):1033–8.
81. Li D, Liu CM, Luo R, Sadakane K, Lam TW. MEGAHIT: an ultra-fast single-node solution for large and complex metagenomics assembly via succinct de Bruijn graph. Bioinformatics. 2015;31(10):1674–6.
82. Nishimura Y, Yoshida T, Kuronishi M, Uehara H, Ogata H, Goto S. ViPTree: the viral proteomic tree server. Bioinformatics. 2017;33(15):2379–80.
83. Moraru C. VirClust-a tool for hierarchical clustering, core protein detection and annotation of (Prokaryotic) viruses. Viruses. 2023;15(4):1007.
84. Rutherford K, Parkhill J, Crook J, Horsnell T, Rice P, Rajandream MA, Barrell B. Artemis: sequence visualization and annotation. Bioinformatics. 2000;16(10):944–5.
85. Grant JR, Enns E, Marinier E, Mandal A, Herman EK, Chen CY, et al. Proksee: in-depth characterization and visualization of bacterial genomes. Nucleic Acids Res. 2023;51(W1):W484–92.
86. Camargo AP, Nayfach S, Chen IA, Palaniappan K, Ratner A, Chu K, et al. IMG/VR v4: an expanded database of uncultivated virus genomes within a framework of extensive functional, taxonomic, and ecological metadata. Nucleic Acids Res. 2023;51(D1):D733–43.
87. Brum J. Using ImageJ to measure viral dimensions in micrographs. 2011. https://cpb-us-w2.wpmucdn.com/u.osu.edu/dist/e/20087/files/2015/08/Using_ImageJ_to_Measure_Viral_Dimensions_in_Micrographs-1ox7nk7.pdf. Accessed 10 Jan 2023.
88. Motulsky HJ, Brown RE. Detecting outliers when fitting data with nonlinear regression-a new method based on robust nonlinear regression and the false discovery rate. BMC Bioinformatics. 2006;7(1):123.
89. Kang I, Jang H, Cho J-C. Complete genome sequences of two *Persicivirga* bacteriophages, P12024S and P12024L. J Virol. 2012;86(16):8907–8.
90. Pooley HM, Abellan FX, Karamata D. A conditional-lethal mutant of *Bacillus subtilis* 168 with a thermosensitive glycerol-3-phosphate cytidylyltransferase, an enzyme specific for the synthesis of the major wall teichoic acid. J Gen Microbiol. 1991;137(4):921–8.
91. Rice C, Harrison W, Kirkpatrick K, Brown E. Cryoprotection from bacterial teichoic acid. SPIE; 2009.
92. Rice CV, Middaugh A, Wickham JR, Friedline A, Thomas KJ 3rd, Scull E, et al. Bacterial lipoteichoic acid enhances cryosurvival. Extremophiles. 2015;19(2):297–305.
93. Das R, Rahlff J. Phage genome architecture and GC content: structural genes and where to find them. bioRxiv. 2024:2024.06.05.597531.
94. Bartlau N, Wichels A, Krohne G, Adriaenssens EM, Heins A, Fuchs BM, et al. Highly diverse flavobacterial phages isolated from North Sea spring blooms. ISME J. 2022;16(2):555–68.
95. Hoetzinger M, Nilsson E, Arabi R, Osbeck CMG, Pontiller B, Hutinet G, et al. Dynamics of Baltic Sea phages driven by environmental changes. Environ Microbiol. 2021;23(8):4576–94.
96. Wait BR, Nokes R, Webster-Brown JG. Freeze-thaw dynamics and the implications for stratification and brine geochemistry in meltwater ponds on the McMurdo Ice Shelf, Antarctica. Antarct Sci. 2009;21(3):243–54.
97. Xu D, Kong H, Yang EJ, Li X, Jiao N, Warren A, et al. Contrasting community composition of active microbial eukaryotes in melt ponds and sea water of the Arctic Ocean revealed by high throughput sequencing. Front Microbiol. 2020;11:1170.
98. Brinkmeyer R, Glöckner F-O, Helmke E, Amann R. Predominance of β-proteobacteria in summer melt pools on Arctic pack ice. Limnol Oceanogr. 2004;49(4):1013–21.
99. Han D, Kang I, Ha HK, Kim HC, Kim OS, Lee BY, et al. Bacterial communities of surface mixed layer in the Pacific sector of the western Arctic Ocean during sea-ice melting. PLoS One. 2014;9(1):e86887.
100. Boetius A, Anesio AM, Deming JW, Mikucki JA, Rapp JZ. Microbial ecology of the cryosphere: sea ice and glacial habitats. Nat Rev Microbiol. 2015;13(11):677–90.
101. Llorens C, Soriano B, Krupovic M, Ictv RC. ICTV virus taxonomy profile: Metaviridae. J Gen Virol. 2020;101(11):1131–2.
102. Alarcon-Schumacher T, Guajardo-Leiva S, Martinez-Garcia M, Diez B. Ecogenomics and adaptation strategies of Southern Ocean viral communities. mSystems. 2021;6(4):e0039621.
103. Sanguino L, Franqueville L, Vogel TM, Larose C. Linking environmental prokaryotic viruses and their host through CRISPRs. FEMS Microbiol Ecol. 2015;91(5):fiv046.
104. Mangiagalli M, Bar-Dolev M, Tedesco P, Natalello A, Kaleda A, Brocca S, et al. Cryo-protective effect of an ice-binding protein derived from Antarctic bacteria. FEBS J. 2017;284(1):163–77.
105. Raymond JA, Fritsen C, Shen K. An ice-binding protein from an Antarctic sea ice bacterium. FEMS Microbiol Ecol. 2007;61(2):214–21.
106. Brauge T, Sadovskaya I, Faille C, Benezech T, Maes E, Guerardel Y, Midelet-Bourdin G. Teichoic acid is the major polysaccharide present in the *Listeria monocytogenes* biofilm matrix. FEMS Microbiol Lett. 2016;363(2):fnv229.
107. Michaud JM, Thompson LR, Kaul D, Espinoza JL, Richter RA, Xu ZZ, et al. Taxon-specific aerosolization of bacteria and viruses in an experimental ocean-atmosphere mesocosm. Nat Commun. 2018;9(1):2017.
108. Baylor ER, Baylor MB, Blanchard DC, Syzdek LD, Appel C. Virus transfer from surf to wind. Science. 1977;198(4317):575–80.
109. Blanchard DC. Jet drop enrichment of bacteria, virus, and dissolved organic material. Pure Appl Geophys. 1978;116(2–3):302–8.
110. Chen M, Xing Y, Kong J, Wang D, Lu Y. Bubble manipulates the release of viral aerosols in aeration. J Hazard Mater. 2024;461:132534.
111. Rahlff J, Wietz M, Giebel HA, Bayfield O, Nilsson E, Bergstrom K, et al. Ecogenomics and cultivation reveal distinctive viral-bacterial communities in the surface microlayer of a Baltic Sea slick. ISME Commun. 2023;3(1):97.
112. Cunliffe M, Whiteley AS, Newbold L, Oliver A, Schafer H, Murrell JC. Comparison of bacterioneuston and bacterioplankton dynamics during a phytoplankton bloom in a fjord mesocosm. Appl Environ Microbiol. 2009;75(22):7173–81.
113. Rahlff J, Stolle C, Giebel HA, Brinkhoff T, Ribas-Ribas M, Hodapp D, Wurl O. High wind speeds prevent formation of a distinct bacterioneuston community in the sea-surface microlayer. FEMS Microbiol Ecol. 2017;93(5):fix041.
114. Brum JR, Hurwitz BL, Schofield O, Ducklow HW, Sullivan MB. Seasonal time bombs: dominant temperate viruses affect Southern Ocean microbial dynamics. ISME J. 2016;10(2):437–49.
115. Evans C, Brussaard CP. Regional variation in lytic and lysogenic viral infection in the Southern Ocean and its contribution to biogeochemical cycling. Appl Environ Microbiol. 2012;78(18):6741–8.
116. Lopez-Simon J, Vila-Nistal M, Rosenova A, De Corte D, Baltar F, Martinez-Garcia M. Viruses under the Antarctic Ice Shelf are active and potentially involved in global nutrient cycles. Nat Commun. 2023;14(1):8295.
117. Jiang SC, Paul JH. Occurrence of lysogenic bacteria in marine microbial communities as determined by prophage induction. Mar Ecol Prog Ser. 1996;142(1–3):27–38.
118. Williamson SJ, Paul JH. Environmental factors that influence the transition from lysogenic to lytic existence in the φHSIC/*Listonella pelagia* marine phage–host system. Microb Ecol. 2006;52(2):217–25.
119. Zhang Z, Liu L, Liu C, Cai W. Studies on the sea surface microlayer. II. The layer of sudden change of physical and chemical properties. J Colloid Interface Sci. 2003;264(1):148–59.
120. Gassen L, Badewien TH, Ewald J, Ribas-Ribas M, Wurl O. Temperature and salinity anomalies in the sea surface microlayer of the South Pacific during precipitation events. J Geophys Res-Oceans. 2023;128(6):e2023JC019638.
121. Rahlff J, Ribas-Ribas M, Brown SM, Mustaffat NIH, Renz J, Peck MA, et al. Blue pigmentation of neustonic copepods benefits exploitation of a prey-rich niche at the air-sea boundary. Sci Rep. 2018;8(1):1–6.
122. Cronin MF, Gentemann CL, Edson J, Ueki I, Bourassa M, Brown S, et al. Air-sea fluxes with a focus on heat and momentum. Front Mar Sci. 2019;6:430.
123. Fairall CW, Bradley EF, Godfrey JS, Wick GA, Edson JB, Young GS. Cool-skin and warm-layer effects on sea surface temperature. J Geophys Res Oceans. 1996;101(C1):1295–308.

Publisher's Note

Springer Nature remains neutral with regard to jurisdictional claims in published maps and institutional affiliations.